LETTER

doi:10.1038/nature11028

Optogenetic stimulation of a hippocampal engram activates fear memory recall

Xu Liu[1]*, Steve Ramirez[1]*, Petti T. Pang[1], Corey B. Puryear[1], Arvind Govindarajan[1], Karl Deisseroth[2] & Susumu Tonegawa[1]

A specific memory is thought to be encoded by a sparse population of neurons[1,2]. These neurons can be tagged during learning for subsequent identification[3] and manipulation[4–6]. Moreover, their ablation or inactivation results in reduced memory expression, suggesting their necessity in mnemonic processes. However, the question of sufficiency remains: it is unclear whether it is possible to elicit the behavioural output of a specific memory by directly activating a population of neurons that was active during learning. Here we show in mice that optogenetic reactivation of hippocampal neurons activated during fear conditioning is sufficient to induce freezing behaviour. We labelled a population of hippocampal dentate gyrus neurons activated during fear learning with channelrhodopsin-2 (ChR2)[7,8] and later optically reactivated these neurons in a different context. The mice showed increased freezing only upon light stimulation, indicating light-induced fear memory recall. This freezing was not detected in non-fear-conditioned mice expressing ChR2 in a similar proportion of cells, nor in fear-conditioned mice with cells labelled by enhanced yellow fluorescent protein instead of ChR2. Finally, activation of cells labelled in a context not associated with fear did not evoke freezing in mice that were previously fear conditioned in a different context, suggesting that light-induced fear memory recall is context specific. Together, our findings indicate that activating a sparse but specific ensemble of hippocampal neurons that contribute to a memory engram is sufficient for the recall of that memory. Moreover, our experimental approach offers a general method of mapping cellular populations bearing memory engrams.

An important question in neuroscience is how a distinct memory is formed and stored in the brain. Recent studies indicate that defined populations of neurons correspond to a specific memory trace[1], suggesting a cellular correlate of a memory engram. Selective ablation or inhibition of such neuronal populations erased the fear memory response[5,6], indicating that these cells are necessary for fear memory expression. However, to prove that a cell population is the cellular basis of a specific fear memory engram it is necessary to conduct a mimicry experiment to show that direct activation of such a population is sufficient for inducing the associated behavioural output[9,10].

The hippocampus is thought to be critical in the formation of the contextual component of fear memories[11–14]. Modelling[15] and experimental[16,17] studies have demonstrated an essential role of the dentate gyrus (DG) of the hippocampus in discriminating between similar contexts. Cellular studies of immediate early gene expression showed that sparse populations of DG granule cells (2–4%) are activated in a given context[18]. Moreover, although the same population of DG granule cells is activated repeatedly in the same environment, different environments[19] or different tasks[20] activate different populations of DG granule cells. These lines of evidence point to the DG as an ideal target for the formation of contextual memory engrams that represent discrete environments.

To label and reactivate a subpopulation of DG cells active during the encoding of a memory, we targeted the DG of c-fos-tTA transgenic mice[3] with the AAV_9-TRE-ChR2-EYFP virus and an optical fibre implant (Fig. 1a). This approach directly couples the promoter of *c-fos*, an immediate early gene often used as a marker of recent neuronal activity[21], to the tetracycline transactivator (tTA), a key component of the doxycycline (Dox) system for inducible expression of a gene of interest[22]. In our system, the presence of Dox inhibits *c-fos*-promoter-driven tTA from binding to its target tetracycline-responsive element (TRE) site, which in turn prevents it from driving ChR2–EYFP (enhanced yellow fluorescent protein) expression. In the absence of Dox, training-induced neuronal activity selectively labels active c-Fos-expressing DG neurons with ChR2–EYFP, which can then be reactivated by light stimulation during testing (Fig. 1b, c). We confirmed that our manipulation restricts the expression of ChR2–EYFP largely to the DG area of the hippocampus (Fig. 1d–g).

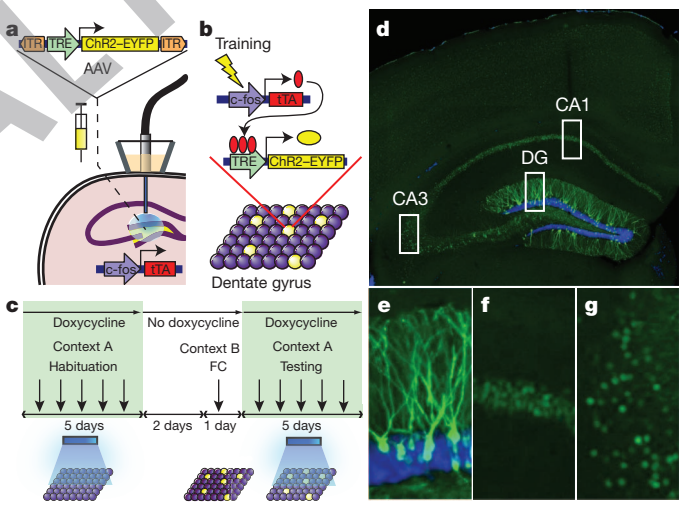

Figure 1 | Basic experimental protocols and selective labelling of DG cells by ChR2–EYFP. **a**, The c-fos-tTA mouse was injected with AAV_9-TRE-ChR2-EYFP and implanted with an optical fibre targeting the DG. **b**, When off Dox, training induces the expression of tTA, which binds to TRE and drives the expression of ChR2–EYFP, labelling a subpopulation of activated cells (yellow) in the DG. **c**, Basic experimental scheme. Mice were habituated in context A with light stimulation while on Dox for 5 days, then taken off Dox for 2 days and fear conditioned (FC) in context B. Mice were put back on Dox and tested for 5 days in context A with light stimulation. **d**, Representative image showing the expression of ChR2–EYFP in a mouse that was taken off Dox for 2 days and underwent FC training. **e**–**g**, An image of each rectangular area in **d** is magnified, showing the DG (**e**), CA1 (**f**) and CA3 (**g**). The green signal from ChR2–EYFP in the DG spreads throughout entire granule cells, including dendrites (**e**), whereas the green signal confined to the nuclei in CA1 and CA3 is due to a 2-h half-life EGFP (shEGFP) expression from the c-fos-shEGFP construct of the transgenic mouse (**f**, **g**). Blue is nuclear marker 4′,6-diamidino-2-phenylindole (DAPI). Panel **d** is at ×10 magnification and panels **e**–**g** are at ×50 magnification.

[1]RIKEN-MIT Center for Neural Circuit Genetics at the Picower Institute for Learning and Memory, Department of Biology and Department of Brain and Cognitive Sciences, Massachusetts Institute of Technology, Cambridge, Massachusetts 02139, USA. [2]Department of Bioengineering and Department of Psychiatry and Behavioral Sciences, Stanford University, Stanford, California 94305, USA.
*These authors contributed equally to this work.

First, to characterize the inducible and activity-dependent expression of ChR2–EYFP, we examined its expression timeline under various treatments (Fig. 2a–h). We observed a complete absence of ChR2–EYFP expression in DG neurons while mice were on Dox (Fig. 2a). Two days off Dox was sufficient to induce ChR2–EYFP expression in home-caged mice (Fig. 2b). The number of ChR2–EYFP-positive cells increased substantially in response to 2 days off Dox followed by fear conditioning (FC; Fig. 2c). We found that the vast majority of c-Fos-positive cells were also ChR2–EYFP positive (Supplementary Fig. 1), confirming that activity-dependent labelling with ChR2–EYFP recapitulated the induction of endogenous c-Fos. A similar increase in ChR2–EYFP expression was seen in a group of mice that were exposed to the same context and tone as the FC group but had no shocks delivered (NS; Fig. 2d). ChR2–EYFP expression lasted at least 5 days (Fig. 2e) and was gone by 30 days (Fig. 2f). Kainic-acid-induced seizures resulted in complete labelling of DG cells with ChR2–EYFP (Fig. 2g), indicating that the relatively sparse labelling in the FC or NS groups was not due to the low infection rate of the virus, but reflected the naturally low activity of DG neurons during the training sessions[18,23]. Notably, NS and FC treatments resulted in similar proportions of ChR2–EYFP-positive cells (Fig. 2h). ChR2–EYFP expression after FC seemed to be restricted to the excitatory neurons, as no overlap was detected between ChR2–EYFP-positive neurons and GABA-positive inhibitory neurons (Supplementary Fig. 2).

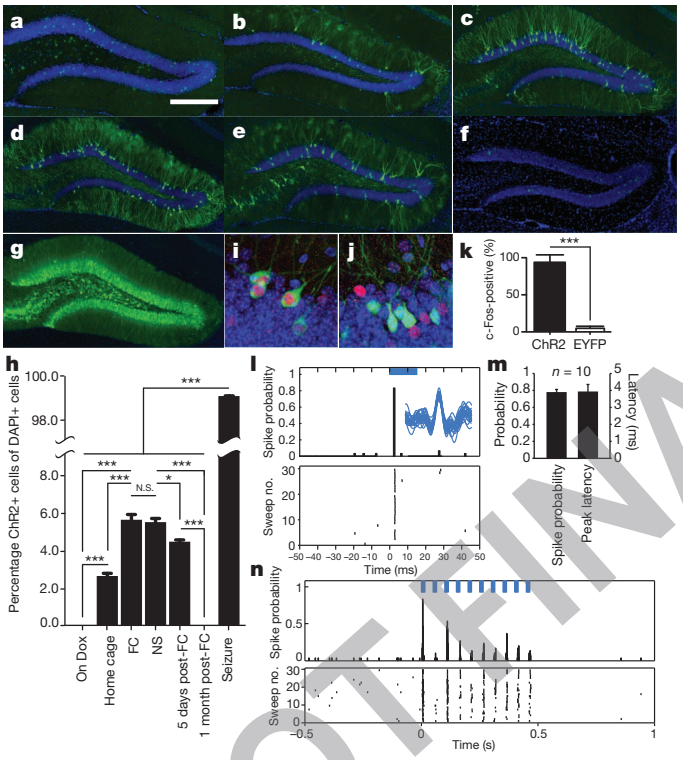

Figure 2 | Activity-dependent expression and stimulation of ChR2–EYFP. **a**–**g**, Representative images of the DG from c-fos-tTA mice injected with AAV_9-TRE-ChR2-EYFP and killed after the following treatments: on Dox (**a**); off Dox for 2 days in home cage (**b**); same as **b** followed by FC (**c**); same as **c** except no shock was delivered (NS; **d**); same as **c**, 5 days after training (**e**); same as **c**, 30 days after training (**f**); same as **b** followed by kainic acid injection to induce seizure (**g**). Residual green signal in **a** and **f** is from nuclear-localized c-fos-shEGFP (see Fig. 1 legend). **h**, Percentage of ChR2–EYFP-positive cells after various treatments represented by **a**–**g** ($n = 5$ subjects each; $F_{6,28} = 94.43$, $^*P < 0.05$; $^{***}P < 0.001$). N.S., not significant. **i**, **j**, Representative DG cells after light stimulation in c-fos-tTA mice injected with AAV_9-TRE-ChR2-EYFP (**i**) or AAV_9-TRE-EYFP (**j**). **k**, Percentage of c-Fos-positive cells among ChR2–EYFP-positive cells or EYFP-positive cells after light stimulation ($n = 3$ subjects each; $^{***}P < 0.001$). **l**, Light-evoked single unit activity of a DG neuron from a c-fos-tTA mouse injected with AAV_9-TRE-ChR2-EYFP. Peri-event histogram (top) and raster plot (bottom) show reliable and precisely time-locked spiking relative to the onset of 15 ms light pulses (blue bar). Inset shows an overlay of waveforms for all the spikes during light stimulation. **m**, Spike probability and peak latency for all the light-responsive cells ($n = 10$) recorded as in **l**. **n**, Multi-unit activity in the DG from a c-fos-tTA mouse injected with AAV_9-TRE-ChR2-EYFP in response to trains of 10 light pulses (15 ms; blue bars) at 20 Hz. Scale bar in **a**, 250 μm. Panels **a**–**g** are at ×10 magnification and panels **i**, **j** are at ×80 magnification. Error bars show mean ± s.e.m.

We injected c-fos-tTA mice with either AAV_9-TRE-ChR2-EYFP or AAV_9-TRE-EYFP, subjected them to FC while off Dox, and then put them back on Dox to test for light-evoked responses from DG cells the following day. The mice were anaesthetized for *in vivo* recordings, and blue light pulses (473 nm, 0.1 Hz, 15 ms pulse duration) were delivered to the DG. Consistent with the sparse labelling of DG neurons (Fig. 2h), we identified only ten DG neurons that responded to light stimulation from nine c-fos-tTA mice injected with AAV_9-TRE-ChR2-EYFP (the ChR2 group). In these neurons, we detected a reliable increase of spike probability precisely time-locked to the onset of light pulses (Fig. 2l, m). These cells also showed robust responses to trains of 20 Hz light stimulation, with a slight decrease in spike probability over time that remained higher above baseline (Fig. 2n). We did not find any light-responsive cells in the ten c-fos-tTA mice injected with AAV_9-TRE-EYFP (the EYFP group; data not shown). Most of the ChR2–EYFP-positive cells in the ChR2 group of mice were also positive for endogenous c-Fos after optical stimulation, although not all c-Fos-positive cells expressed ChR2–EYFP. Very few neurons expressing EYFP in the EYFP group of mice were c-Fos positive (Fig. 2i–k and Supplementary Fig. 3). The proportion of c-Fos-positive cells in the downstream CA3 region was greater in the ChR2 group compared with the EYFP group after optical stimulation of DG neurons, and this number was comparable to the proportion of CA3 c-Fos-positive cells obtained by exposing a separate group of mice to the conditioned context after FC (Supplementary Fig. 4).

Next, we tested whether activating a population of DG neurons labelled by ChR2–EYFP during the encoding of a fear memory was sufficient for memory recall. The experimental group (Exp) consisted of c-fos-tTA mice unilaterally injected with AAV_9-TRE-ChR2-EYFP and implanted with an optical fibre targeting the DG (Fig. 1a). Mice were kept on Dox and underwent 5 days of habituation to record their basal level of freezing in one context (context A) during both light-off and light-on epochs. Next, they were taken off Dox and underwent FC in a distinct chamber (context B) in which a tone was paired with shock. The mice were then subjected to 5 days of testing with light-off and light-on epochs in context A while on Dox (Fig. 1c). During the habituation sessions, the Exp mice showed very little freezing during either light-off or light-on epochs. In contrast, after FC, freezing levels during light-on epochs were higher compared with light-off epochs, which indicated light-induced fear memory recall (Fig. 3a). Increased freezing during light-on epochs was observed over all 5 days of test sessions with no discernible day-dependent difference (Supplementary Fig. 5g). These data suggest that DG cells that express endogenous c-Fos during training, and therefore become labelled by ChR2–EYFP, define an active neural population that is sufficient for memory recall upon subsequent reactivation.

To rule out the possibility that post-training freezing by optical stimulation was due to the activation of DG cells unrelated to fear learning, we injected another group of mice (NS) with AAV_9-TRE-ChR2-EYFP and administered the same habituation, training, and test sessions as the Exp group, except that no shock was delivered during the training session. Despite the fact that a similar level of ChR2–EYFP expression was detected in the NS group compared with the Exp group, both in terms of proportion of cells labelled (Fig. 2h) and ChR2–EYFP fluorescence intensity per cell (Supplementary Fig. 6), light did not induce post-training freezing in the NS group (Fig. 3b). This indicates that the freezing observed in the Exp group requires optical activation of a specific subset of ChR2–EYFP-positive DG cells

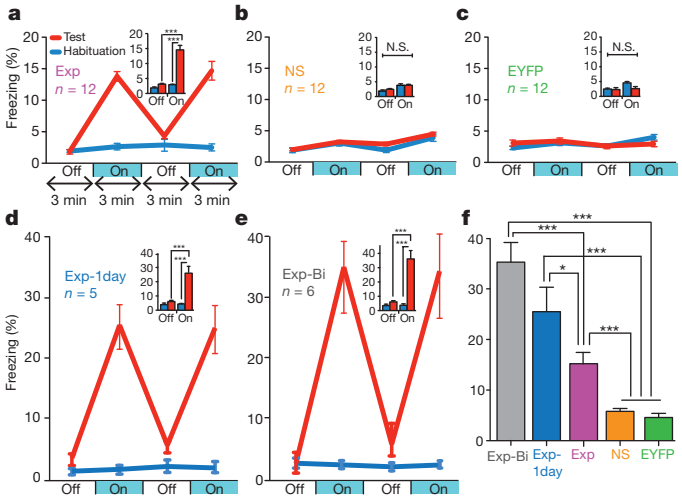

Figure 3 | Optical stimulation of engram-bearing cells induces post-training freezing. **a**, c-fos-tTA mice injected with AAV$_9$-TRE-ChR2-EYFP and trained with FC (Exp group) show increased freezing during 3-min light-on epochs. Freezing for each epoch represents 5-day average (Supplementary Fig. 5a, g). Freezing levels for the two light-off and light-on epochs are further averaged in the inset ($n = 12$, $F_{1,22} = 37.98$, $^{***}P < 0.001$). **b**, Mice trained similarly to the conditions in **a** but without foot shock (NS group) do not show increased light-induced freezing ($n = 12$). N.S., not significant. **c**, Mice injected with AAV$_9$-TRE-EYFP and trained with FC (EYFP group) do not show increased light-induced freezing ($n = 12$). **d**, Mice trained similarly to the conditions in **a** but kept off Dox for 1 day before FC training (Exp-1day group) showed greater freezing during test light-on epochs compared to Exp group ($n = 5$, $F_{1,8} = 38.26$, $^{***}P < 0.001$). **e**, Mice trained similarly to the conditions in **a** but bilaterally injected with AAV$_9$-TRE-ChR2-EYFP and implanted with optical fibres (Exp-Bi group) showed even higher levels of freezing during test light-on epochs ($n = 6$, $F_{1,10} = 85.14$, $^{***}P < 0.001$). **f**, Summary of freezing levels of the five groups during test light-on epochs ($F_{4,42} = 37.62$, $^{*}P < 0.05$; $^{***}P < 0.001$). Error bars show mean ± s.e.m.

that are associated with FC and that activating a population of DG cells not associated with FC does not induce freezing. Yet another group of mice (EYFP) were injected with AAV$_9$-TRE-EYFP and underwent identical habituation, training, and testing sessions as the Exp group. The proportion of cells expressing EYFP was comparable to that seen in the Exp group expressing ChR2–EYFP (Supplementary Fig. 7). However, the EYFP group did not show increased post-training freezing (Fig. 3c). This result rules out the possibility that increased freezing in the Exp group was due to any non-specific effects of post-training optical stimulation.

The light-induced freezing levels of the Exp group were relatively low (~15%) compared with those typically reported from exposure to a conditioned context (~60%)[3]. One possibility is that light activation of background-activity-induced ChR2–EYFP (Fig. 2b) interfered with the expression of the specific fear memory. We confirmed that limiting the off-Dox period from 2 days to 1 day reduced the background expression of ChR2–EYFP by at least twofold (compare Supplementary Fig. 8a home cage with Fig. 2h home cage). A group of mice (Exp-1day) that went through the same design outlined in Fig. 1c but with this modification showed greater freezing levels (~25%) during the light-on epoch of test sessions compared to the Exp group (Fig. 3d, f). Another possible factor contributing to the modest light-induced freezing in the Exp group may be the limited number of cells optically stimulated. To test this possibility, we bilaterally injected a group of mice (Exp-Bi) with AAV$_9$-TRE-ChR2-EYFP and bilaterally implanted optical fibres targeting the DG, and then subjected these mice to the same scheme as that shown in Fig. 1c. During the light-on epochs of the test sessions, the Exp-Bi group exhibited levels of freezing (~35%) that were almost as high as those induced by the conditioned context (Fig. 3e, f, Supplementary Fig. 9 and Supplementary Movies).

We next examined whether the light-induced fear memory recall was context specific. First, to test whether two different contexts activate similar or distinct populations of DG cells, we took the mice off Dox for 2 days and then exposed them to a novel context (context C, an open field) to label the active DG cells with ChR2–EYFP. After being put back on Dox, the mice were fear conditioned in a different context (context B) and killed 1.5 h later (Fig. 4a). The expression of ChR2–EYFP was used to identify cells previously activated in context C whereas endogenous c-Fos was used to identify cells recently activated in context B. Immunohistochemical analyses revealed a chance level of overlap between ChR2–EYFP-positive and c-Fos-positive cells, suggesting that two independent DG cell populations were recruited for the representation of the two distinct contexts (Fig. 4b–g). To test the context specificity of light-induced recall of a fear memory, we subjected a new group of mice (an open field fear-conditioned group; OF-FC) to habituation sessions in context A, followed by 2 days off Dox and exposure to context C to label neurons active in context C with ChR2–EYFP. Next, we put the mice back on Dox and performed FC in context B (Fig. 4h). These mice were then placed back in context A and tested for light-induced freezing. Light failed to evoke an increase in freezing responses (Fig. 4i). Similarly low levels of freezing were observed in another group of mice (FC-OF) in which FC in context B while on Dox preceded exposure to context C while off Dox (Supplementary Fig. 10). Together, these results indicate that light

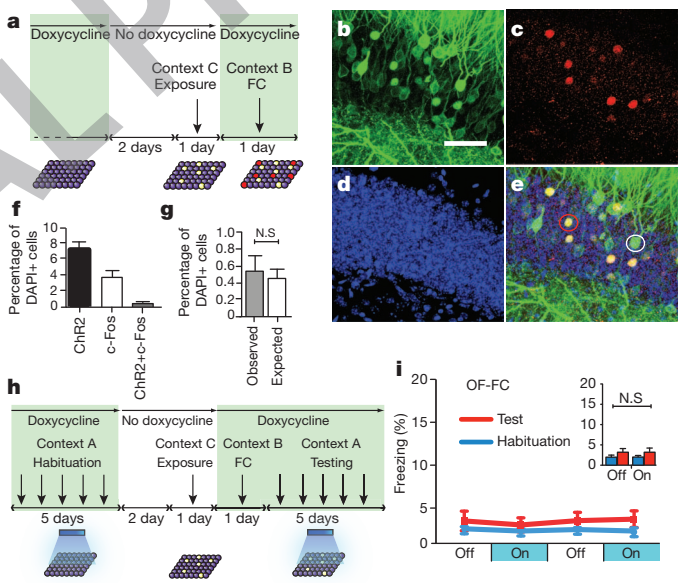

Figure 4 | Labelling and stimulation of independent DG cell populations. **a**, c-fos-tTA mice injected with AAV$_9$-TRE-ChR2-EYFP were taken off Dox and exposed to context C to label activated cells with ChR2–EYFP (yellow), then put back on Dox and trained with FC in context B to activate endogenous c-Fos (red). **b**–**e**, Representative images of DG from these mice are shown. **b**, ChR2–EYFP-labelled cells activated in context C. **c**, c-Fos-labelled cells activated in context B. **d**, Nuclear marker DAPI. **e**, Merge. The white and red circles show examples of ChR2–EYFP-positive and c-Fos-positive cells, respectively. The c-Fos-positive cells in **e** appear yellow because they express both endogenous c-Fos (red) and the nuclear-localized c-fos-shEGFP (green) (see Fig. 1 legend). **f**, Percentage of ChR2–EYFP-positive, endogenous c-Fos-positive, and double-positive cells among total cells (DAPI+) ($n = 5$). **g**, The observed percentage of double-positive cells is the same as what would be expected if the two cell populations were independent (that is, a product of the observed percentage of ChR2–EYFP single-positive and c-Fos single-positive cells). **h**, Behaviour setup for mice exposed to an open field in context C while off Dox and subsequently fear conditioned in context B while on Dox (OF-FC). **i**, OF-FC mice ($n = 5$) do not show increased light-induced freezing. N.S., not significant. Panels **b**–**e** are at ×80 magnification. Scale bar in **b**, 10 μm. Error bars show mean ± s.e.m.

reactivation of cells labelled in context C did not induce fear memory recall associated with context B.

We have shown that optical activation of hippocampal cells that were active during FC elicits freezing behaviour. To our knowledge, this is the first demonstration that directly activating a subset of cells involved in the formation of a memory is sufficient to induce the behavioural expression of that memory. Our results and previous studies that addressed the necessity of similarly sparse cell populations in the amygdala[5,6] argue that defined cell populations can form a cellular basis for fear memory engrams. The memory engram that we selectively labelled and manipulated is probably contextual in nature, as previous studies have demonstrated that hippocampal interventions affect conditioned freezing responses to a context but not a tone[12,13,24]. Indeed, recent findings show that optogenetic inhibition of the hippocampal CA1 region during training or testing inhibited the recall of a contextual fear memory, while leaving auditory-cued fear memory recall intact[25]. However, we cannot completely rule out the possibility that the fear memory recalled in our experiments may have some tone memory component.

Our observation that freezing responses were elicited by optical stimulation in the experimental groups (Exp, Exp-1day and Exp-Bi), but not in the OF-FC or FC-OF group, strongly supports a dual memory engram hypothesis of contextual FC[26–28]. In this hypothesis, hippocampal cells are recruited to form contextual memory engrams, but these contextual engrams alone do not represent a complete fear memory. For a fear memory to be formed, the information from the contextual memory engram must be transferred to the basolateral amygdala coincidentally with the information representing a foot shock. In the OF-FC or FC-OF scheme, two distinct contextual memory engrams were formed in the DG, which were represented by two distinct sets of DG cells. One of these two contextual engrams (the one for context B) was associated with the representation of the shock, but not the other engram (the one for context C). Because only the latter, but not the former, was labelled by ChR2, optical stimulation could not elicit fear memory expression.

Although we have demonstrated the sufficiency of a DG memory engram for the behavioural expression of a fear memory, we cannot conclude that this engram is necessary for behavioural recall. During contextual FC, it is likely that multiple contextual memory engrams are formed in a series of hippocampal regions. Each of these engrams may contribute to the formation of the complete fear memory in the BLA and may also be capable of reactivating it independently, as we observed in the case of the DG engrams. Because the hippocampus is not a linear feed-forward network but contains several parallel circuits, inhibiting the formation or activation of contextual engrams in one region may not necessarily block the expression of the fear memory. For instance, disruption of contextual memory engrams in the DG could be circumvented by CA1 engrams, which could be generated through the direct input from the entorhinal cortex and may be sufficient to activate the fear memory engram in the BLA. Indeed, we recently generated a mouse mutant, which permitted us to demonstrate that the DG input to the CA3 is dispensable in the formation and retrieval of contextual fear memory[17].

The approach and methods described in this work will be a powerful tool for mapping multiple component engrams, each contributing to an overall memory. A multifaceted analysis of these engrams and their interplay will reveal the nature of the overall memory engram.

METHODS SUMMARY

Virus-mediated gene expression. The pAAV-TRE-ChR2-EYFP and pAAV-TRE-EYFP plasmids were constructed by standard methods and packed as AAV_9 viruses. The viruses were stereotaxically injected into the DG (0.15 µl).

Immunohistochemistry. Mice were killed after various treatments and brain slices were prepared for immunohistochemistry and confocal microscopy. Coronal sections were immunostained for EYFP and/or c-Fos. All imaging and analyses were performed blind to the experimental conditions.

***In vivo* recording.** An optrode consisting of a tungsten electrode glued to a 200 µm optical fibre coupled to a 473 nm laser was used for optical stimulation and extracellular electrical recordings in head-fixed, isoflurane-anaesthetized mice.

Behavioural tests. Mice used for behavioural tests were injected with AAV_9 virus and implanted with an optical fibre targeting the DG. All mice were habituated in context A while on 40 mg kg^{-1} Dox for 5 days for 12 min per day with light stimulation (473 nm, 20 Hz, 15 ms) during minutes 4–6 and 10–12. The groups of mice were taken off Dox for 1 (Exp-1day) or 2 days (Exp, Exp-Bi, EYFP and NS) and fear conditioned in context B with a tone, with (Exp, Exp-1day, Exp-Bi and EYFP) or without (NS) shock. The OF-FC group was taken off Dox for 2 days and exposed to context C without shock, then fear conditioned in context B while on Dox. The FC-OF group was fear conditioned in context B while on Dox, then taken off Dox for 2 days and exposed to context C without shock. All groups were put back on Dox and tested in context A for 5 days in a manner similar to that used in the habituation sessions. All groups except the NS group were then put back to context B for a contextual fear probe trial 1 day after the last light stimulation, followed by a cued tone probe trial in context D the next day. Freezing levels were scored by experimenters blind to all treatment conditions.

Full Methods and any associated references are available in the online version of the paper at www.nature.com/nature.

Received 1 November 2011; accepted 15 March 2012.
Published online 22 March 2012.

1. Josselyn, S. A. Continuing the search for the engram: examining the mechanism of fear memories. *J. Psychiatry Neurosci.* **35,** 221–228 (2010).
2. Silva, A. J. *et al.* Molecular and cellular approaches to memory allocation in neural circuits. *Science* **326,** 391–395 (2009).
3. Reijmers, L. G., Perkins, B. L., Matsuo, N. & Mayford, M. Localization of a stable neural correlate of associative memory. *Science* **317,** 1230–1233 (2007).
4. Han, J. H. *et al.* Neuronal competition and selection during memory formation. *Science* **316,** 457–460 (2007).
5. Han, J. H. *et al.* Selective erasure of a fear memory. *Science* **323,** 1492–1496 (2009).
6. Zhou, Y. *et al.* CREB regulates excitability and the allocation of memory to subsets of neurons in the amygdala. *Nature Neurosci.* **12,** 1438–1443 (2009).
7. Boyden, E. S. *et al.* Millisecond-timescale, genetically targeted optical control of neural activity. *Nature Neurosci.* **8,** 1263–1268 (2005).
8. Tye, K. M. *et al.* Amygdala circuitry mediating reversible and bidirectional control of anxiety. *Nature* **471,** 358–362 (2011).
9. Martin, S. J. & Morris, R. G. New life in an old idea: the synaptic plasticity and memory hypothesis revisited. *Hippocampus* **12,** 609–636 (2002).
10. Gerber, B., Tanimoto, H. & Heisenberg, M. An engram found? Evaluating the evidence from fruit flies. *Curr. Opin. Neurobiol.* **14,** 737–744 (2004).
11. Lever, C. *et al.* Long-term plasticity in hippocampal place-cell representation of environmental geometry. *Nature* **416,** 90–94 (2002).
12. Phillips, R. G. & LeDoux, J. E. Differential contribution of amygdala and hippocampus to cued and contextual fear conditioning. *Behav. Neurosci.* **106,** 274–285 (1992).
13. Kim, J. J. & Fanselow, M. S. Modality-specific retrograde amnesia of fear. *Science* **256,** 675–677 (1992).
14. Ramamoorthi, K. *et al.* Npas4 regulates a transcriptional program in CA3 required for contextual memory formation. *Science* **334,** 1669–1675 (2011).
15. Treves, A. & Rolls, E. T. Computational analysis of the role of the hippocampus in memory. *Hippocampus* **4,** 374–391 (1994).
16. McHugh, T. J. *et al.* Dentate gyrus NMDA receptors mediate rapid pattern separation in the hippocampal network. *Science* **317,** 94–99 (2007).
17. Nakashiba, T. *et al.* Young dentate granule cells mediate pattern separation whereas old granule cells facilitate to pattern completion. *Cell*, (2012).
18. Schmidt, B., Marrone, D. F. & Markus, E. J. Disambiguating the similar: The dentate gyrus and pattern separation. *Behav. Brain Res.* **226,** 56–65 (2012).
19. Chawla, M. K. *et al.* Sparse, environmentally selective expression of *Arc* RNA in the upper blade of the rodent fascia dentata by brief spatial experience. *Hippocampus* **15,** 579–586 (2005).
20. Satvat, E. *et al.* Changes in task demands alter the pattern of *zif268* expression in the dentate gyrus. *J. Neurosci.* **31,** 7163–7167 (2011).
21. Kubik, S., Miyashita, T. & Guzowski, J. F. Using immediate-early genes to map hippocampal subregional functions. *Learn. Mem.* **14,** 758–770 (2007).
22. Shockett, P. E. & Schatz, D. G. Diverse strategies for tetracycline-regulated inducible gene expression. *Proc. Natl Acad. Sci. USA* **93,** 5173–5176 (1996).
23. Leutgeb, J. K., Leutgeb, S., Moser, M. B. & Moser, E. I. Pattern separation in the dentate gyrus and CA3 of the hippocampus. *Science* **315,** 961–966 (2007).
24. Lee, I. & Kesner, R. P. Differential contributions of dorsal hippocampal subregions to memory acquisition and retrieval in contextual fear-conditioning. *Hippocampus* **14,** 301–310 (2004).
25. Goshen, I. *et al.* Dynamics of retrieval strategies for remote memories. *Cell* **147,** 678–689 (2011).
26. Seidenbecher, T., Laxmi, T. R., Stork, O. & Pape, H. C. Amygdalar and hippocampal theta rhythm synchronization during fear memory retrieval. *Science* **301,** 846–850 (2003).

27. Schafe, G. E., Doyere, V. & LeDoux, J. E. Tracking the fear engram: the lateral amygdala is an essential locus of fear memory storage. *J. Neurosci.* **25,** 10010–10014 (2005).
28. Rogan, M. T., Staubli, U. V. & LeDoux, J. E. Fear conditioning induces associative long-term potentiation in the amygdala. *Nature* **390,** 604–607 (1997).

Supplementary Information is linked to the online version of the paper at www.nature.com/nature.

Acknowledgements We thank S. Huang, G. Lin, M. Ragion and X. Zhou for help with the experiments, T. Ryan, A. Rivest, J. Young, R. Redondo and G. Dragoi for comments and discussions on the manuscript, and all the members of the Tonegawa laboratory for their support. This work is supported by National Institutes of Health grants R01-MH078821, P50-MH58880 to S.T. and RIKEN Brain Science Institute.

Author Contributions X.L., S.R., A.G. and S.T. contributed to the study design. X.L., S.R. and P.T.P. contributed to the data collection and interpretation. X.L. cloned all constructs. X.L. and S.R. conducted the surgeries and the behaviour experiments. S.R. conducted the expression timeline experiments. P.T.P. conducted the electrophysiology experiments. C.B.P. contributed to the setup of the electrophysiology apparatus and wrote the Matlab software to analyse the data. K.D. provided the original ChR2 construct. X.L., S.R. and S.T. wrote the paper. All authors discussed and commented on the manuscript.

Author Information Reprints and permissions information is available at www.nature.com/reprints. The authors declare no competing financial interests. Readers are welcome to comment on the online version of this article at www.nature.com/nature. Correspondence and requests for materials should be addressed to S.T. (tonegawa@mit.edu).

METHODS

Subjects. The c-fos-tTA mice were generated from TetTag mice by breeding them with C57BL/6J mice and selecting those carrying only the c-fos-tTA transgene and not the bi-cistronic tetO promoter driving tau-LacZ and tTA^{H100Y} transgenes. These mice also contained a separate transgene consisting of a *c-fos* promoter driving the expression of nuclear-localized 2-h half-life EGFP (shEGFP), which is distinct from the whole-cell-localized ChR2–EYFP. Mice had food and water *ad libitum* and were socially housed until the beginning of the surgery. The mice were 8–12 weeks old at the time of surgery and had been raised on food containing 40 mg kg^{-1} Dox for 4 weeks before surgery. Mice were single housed post-surgery and throughout the rest of the experiments. All procedures relating to mouse care and treatment conformed to the institutional and National Institutes of Health guidelines.

Virus construct and packaging. The pAAV-TRE-ChR2-EYFP plasmid was constructed by cloning TRE-ChR2-EYFP into an AAV backbone using the SpeI restriction site at the 5′ terminus and the blunt end at the 3′ terminus of the insert. The pAAV-TRE-EYFP plasmid was constructed by removing the ChR2 fragment from the pAAV-TRE-ChR2-EYFP plasmid using NheI and AgeI restriction sites, blunting with T4 DNA polymerase, and self-ligation of the vector, which retained the ATG start codon of the *EYFP* gene from the *ChR2-EYFP* fusion gene. The recombinant AAV vectors were serotyped with AAV_9 coat proteins and packaged by the Gene Therapy Center and Vector Core at the University of Massachusetts Medical School. Viral titres were 1×10^{13} genome copy ml^{-1} for AAV_9-TRE-ChR2-EYFP and 1.5×10^{13} genome copy ml^{-1} for AAV_9-TRE-EYFP.

Stereotactic injection and optical fibre implant. All surgeries were performed under stereotaxic guidance. Mice were anaesthetized using 500 mg kg^{-1} avertin. The virus was injected using a glass micropipette attached to a 10 µl Hamilton microsyringe (701LT; Hamilton) through a microelectrode holder (MPH6S; WPI) filled with mineral oil. A microsyringe pump (UMP3; WPI) and its controller (Micro4; WPI) were used to control the speed of the injection. The needle was slowly lowered to the target site and remained for 10 min before the beginning of the injection. Mice for timeline studies and head-fixed electrophysiology recordings were injected bilaterally (−2.2 mm anterioposterior (AP); ± 1.3 mm mediolateral (ML); –2.0 mm dorsoventral (DV)[29]) with 0.15 µl AAV_9 virus at a rate of 0.1 µl min^{-1}. After the injection the needle stayed for five additional minutes before it was slowly withdrawn. The mice used for behaviour tests were unilaterally or bilaterally injected with the virus same as described above. After withdrawing of the needle, a Doric patchcord optical fibre (200 µm core diameter; Doric Lenses) precisely cut to the optimal length was lowered above the injection site (–2.2 mm AP; ± 1.3 mm ML; –1.6 mm DV). Three jewelry screws were screwed into the skull surrounding the implant site of each hemisphere to provide extra anchor points. A layer of adhesive cement (C&B Metabond) was applied followed with dental cement (Teets cold cure; A-M Systems) to secure the optical fibre implant. A cap made from the bottom part of a 15 ml Falcon tube (for unilateral implant) or the top part of an Eppendorf tube (for bilateral implant) was inserted to protect the implant and the incision was closed with sutures. Mice were given 1.5 mg kg^{-1} metacam as analgesic and remained on a heating pad until fully recovered from anaesthesia. Mice were allowed to recover for 2 weeks before all subsequent experiments. All fibre placements (Supplementary Fig. 11) and viral injection sites were verified histologically. As criteria we only included mice with ChR2–EYFP expression limited to the DG, which led to the exclusion of two mice throughout the study.

ChR2–EYFP and EYFP expression timeline. Fourteen days after surgery, subjects were either kept on Dox and immediately killed or taken off Dox for 1 or 2 days. The mice from the latter two groups were either killed with no further treatments (home cage), or underwent FC or NS protocols as described in the behaviour section below. After each treatment, mice were killed 1.5 h, 24 h, 5 days or 30 days later, as described in the main text, and underwent immunohistochemistry procedures. For seizure experiments, mice were taken off Dox for 2 days and injected intraperitoneally with 20 mg kg^{-1} kainic acid. The mice were killed 6 h after the first behavioural onset of seizure.

***In vivo* recording.** Mice were anaesthetized by isoflurane inhalation and placed in the stereotactic system with anaesthesia maintained with 0.5–1% isoflurane throughout the recording. An optrode consisting of a tungsten electrode (1 MΩ) glued to an optical fibre (200 µm core diameter; Doric Lenses), with the tip of the electrode extending beyond the tip of the fibre by 500 µm was used for simultaneous optical stimulation and extracellular recordings. The optrode was lowered to the dentate gyrus (−2.2 mm AP; 1.3 mm ML; −2.0 mm DV) using a hydraulic micromanipulator (Model 640; David Kopf Instruments). The optical fibre was connected to a 200 mW 473 nm laser (MBL F473; Opto Engine) and controlled by a function generator (33220A; Agilent Technologies). The power intensity of light emitted from the optrode was calibrated to about 9 mW, which was consistent with the power intensity used in the behavioural assays. To identify ChR2-labelled cells, light pulses of 15 ms were delivered at 0.1 Hz at the recording sites approximately every 5–10 µm throughout the DG. After light responsive cells were detected, two types of light stimuli were tested: 15 ms light pulse every 10 s and a train of ten 15 ms light pulses at 20 Hz every 10 s. Unit activity was band-pass filtered (500 Hz–5 KHz) and acquired with an Axon Digidata 1440A acquisition system running Clampex 10.2 software. Data were analysed with custom software written in Matlab. After the recording, endogenous c-Fos expression was induced by delivering two epochs of 3-min light stimulation (9 mW, 20 Hz, 15 ms), separated by 3 min, to the DG, the same as in behavioural experiments (see below). Mice were killed and perfused 90 min later.

Immunohistochemistry. Mice were overdosed with avertin and perfused transcardially with cold PBS, followed by 4% paraformaldehyde (PFA) in PBS. Brains were extracted from the skulls and kept in 4% PFA at 4 °C overnight. Fifty-micrometre coronal slices were taken using a vibrotome and collected in cold PBS. For immunostaining, each slice was placed in PBST (PBS + 0.2% Triton X-100) with 5% normal goat serum for 1 h and then incubated with primary antibody at 4 °C for 24 h (rabbit anti-c-Fos 1:5,000, Calbiochem; rabbit anti-GABA 1:5,000, Abcam; chicken anti-GFP 1:500, Invitrogen). Slices then underwent three wash steps for 10 min each in PBST, followed by 1 h incubation with secondary antibody (1:200 AlexaFlour488 anti-chicken, Invitrogen; 1:200 AlexFlour568 anti-rabbit, Invitrogen). Slices were then incubated for 15 min with DAPI (1:10,000) and underwent three more wash steps of 10 min each in PBST, followed by mounting and coverslipping on microscope slides.

Cell counting. To characterize the expression timeline of ChR2–EYFP and EYFP, the number of EYFP immunoreactive neurons in the DG were counted from six coronal slices (spaced 120 µm from each other) per mouse ($n = 5$ for ChR2 group, $n = 3$ for EYFP group). Coronal slices were taken from dorsal hippocampus centred on coordinates covered by our optical fibre implants (−1.94 mm to −2.46 mm AP; Supplementary Fig. 11). Confocal fluorescence images were acquired on a Leica TCS SP2 AOBS scanning laser microscope using a ×20/0.70 NA oil immersion objective. The image analysis module Visiomorph DP within VIS (Visiopharm) calculated the number of ChR2–EYFP-positive or EYFP-positive cells per section by thresholding EYFP immunoreactivity above background levels and using DAPI staining to distinguish between nuclei. The analysis module also permitted isolation of only ChR2–EYFP-positive and EYFP-positive neurons by setting size and fluorescence thresholds to filter out nuclear-localized c-fos-shEGFP-positive cells. The cell body layer of DG granule cells was outlined as a region of interest (ROI) according to the DAPI signal in each slice. A similar protocol was followed for c-Fos-positive cell counts in DG and CA3, except a Cy3 filter was applied for the latter. For quantification comparisons, we used a one-way ANOVA followed by Tukey's multiple comparisons using $\alpha = 0.05$. Data were analysed using Microsoft Excel with the Statplus plug-in and Prism (GraphPad Software).

To analyse the overlap between c-Fos and ChR2–EYFP-expressing or EYFP-expressing cells, a z-stack method was used in conjunction with ImageJ[30] to montage ten optical stacks (1 µm each, step size 10 µm) taken under a ×20/0.70 NA oil immersive objective. Separate GFP and Cy3 filtered images were digitally combined to produce composite images. Equal cutoff thresholds were applied to all captures to remove background autoflouresence. All imaging and analyses were performed blind to the experimental conditions. To quantify the expression levels of ChR2–EYFP per cell, an experimenter blind to each condition used ImageJ to calculate the fluorescence intensity signal as integrated density for ten randomly chosen DG cells per hippocampal slice ($n = 3$ slices per mouse, 5 mice per condition; Supplementary Fig. 6).

Behaviour assays. All the behaviour tests were conducted during the light cycle of the day. Four different contexts were used in the behaviour assays. Context A was a 30 × 25 × 33 cm conditioning chamber within a room with black walls, black curtains, and dim lighting. The chamber had a white plastic floor and was scented with 0.25% benzaldehyde. Context B was a 29 × 25 × 22 cm conditioning chamber within a second room with white walls and bright lighting. The chamber had a gridded floor and a triangular roof, and was scented with 1% acetic acid. Context C was a 41 × 41 × 31 cm unscented open field arena within a third room with white walls and intermediate lighting. Context D was a 29 × 25 × 22 cm conditioning chamber in the same room as context C. It had a white acrylic glass floor and was unscented. The experimental groups (Exp, Exp-1day and Exp-Bi) and EYFP control (EYFP) groups underwent exactly the same training protocol. During the habituation session, each mouse was introduced to context A daily for 5 days while on 40 mg kg^{-1} Dox food. Each day the mouse was loaded into the chamber and the optical fibre implant was connected to a 473 nm laser (MBL F473; Opto Engine) controlled by a function generator (33220A; Agilent Technologies). The mouse was then allowed to explore the chamber for 12 min. The 12 min session was divided into four 3-min epochs, with the first and third epoch as the light-off epochs, and the second and fourth epochs as the light-on epochs. During the light-on epochs, the mouse received light stimulation (9 mW, 20 Hz, 15 ms) for the

entire 3-min duration. At the end of the 12 min, the mouse was immediately detached from the laser and returned to its home cage. Following the fifth habituation session, the mouse was kept on regular food without Dox for 1 (Exp-1day) or 2 (Exp, Exp-Bi and EYFP) days until the training session. On the training day the mice received three training trials separated by 3 h in their home cages. For each training trial, the mouse was kept in the conditioning chamber in context B for 500 s. A tone (20 s, 75 dB, 2,000 Hz) was turned on at 180 s, 260 s, 340 s and 420 s, each of which co-terminated with a foot shock (2 s, 0.75 mA). After the third training trial, the mouse was returned to its home cage and placed on food containing 1 g kg^{-1} Dox overnight to rapidly turn off any additional ChR2–EYFP or EYFP expression. The test session started the next day and the mouse was switched back to food containing 40 mg kg^{-1} Dox. The procedure for the 5-day test session was exactly the same as the habituation session in context A. The day after the last test session, the mouse was returned to the original context B and exposed to the chamber for 300 s for a retrieval session to assay contextual fear memory. The next day, the mouse was introduced to context D for cued fear memory retrieval. This session lasted for 780 s, with a tone (60 s, 75 dB, 2,000 Hz) turned on at 180 s, 420 s and 660 s. The no shock (NS) group went through the same habituation, training and test sessions as the Exp group, except that no foot shock was given during the training session. The open field fear-conditioned (OF-FC) group went through the same habituation sessions. After the fifth habituation session, Dox was removed from the mouse's diet for 2 days, followed by exposure to the open field arena in context C to allow for 10 min of active exploration. The mouse was subsequently returned to its home cage and placed on 1 g kg^{-1} Dox food overnight. The following day, the mouse was fear conditioned in context B in the same manner as described above. Test sessions were administered over 5 days in context A on 40 mg kg^{-1} Dox food, and the OF-FC group also underwent context and tone probe trials after the 5 days of testing. The fear-conditioned open field FC-OF) group went through the same habituation sessions. The day after the fifth habituation, the mouse was kept on 40 mg kg^{-1} Dox food and went through the FC procedure in context B as described above. The mouse was placed off Dox for 2 days after FC. Then the mouse was exposed to the open field arena in context C and allowed to freely explore for 10 min, after which the mouse was returned to their home cage with 1 g kg^{-1} Dox food overnight, followed by test sessions over 5 days in context A on 40 mg kg^{-1} Dox food. Freezing behaviour for training, context, and tone probe trials was recorded with a digital camera and measured with FreezeFrame software (ActiMetrics). Light stimulation during the habituation and test sessions interfered with the motion detection of the program, and thus the freezing of these sessions was manually scored. Two experimenters scored each video independently in a double-blinded manner. The overall scores showed a $<3\%$ difference between the two experimenters and for simplicity only one set of scores from one experimenter was reported. The manual scoring and computer scoring of the same training videos gave similar freezing scores. For each group, within each session (habituation and test) and within each epoch (light-on and light-off), a one-way ANOVA with repeated measures followed by Tukey's multiple comparisons ($\alpha = 0.05$) revealed no difference over 5 days (Supplementary Fig. 5). We therefore averaged the freezing level over 5 days for each mouse. A two-way ANOVA with repeated measures followed by Tukey's multiple comparisons ($\alpha = 0.05$) revealed that only the experimental groups (Exp, Exp-1day and Exp-Bi) showed an increase in averaged freezing levels for light-on epochs of test sessions compared to light-off epochs of test sessions and light-on epochs of habituation sessions (Fig. 3a, d, e).

29. Paxinos, G. & Franklin, K. *The Mouse Brain in Stereotaxic Coordinates* (Academic, 2001).
30. Rasband, W. S. Image J. http://imagej.nih.gov/ij/ (National Institutes of Health, 1997–, 2011).